

Real time simulations of scalar fields with kernelled complex Langevin equation

Daniel Alvestad,^a Alexander Rothkopf^a and Dénes Sexty^{b,*}

^a*Faculty of Science and Technology, University of Stavanger,
4021 Stavanger, Norway*

^b*Institute of Physics, NAWI Graz, University of Graz,
Universitätsplatz 5, 8010 Graz, Austria*

E-mail: alexander.rothkopf@uis.no, denes.sexty@uni-graz.at

Real time evolution of a scalar field theory is investigated. The severe sign problem is circumvented using the Complex Langevin equation. The naive application of the method breaks down for extended real times due to the appearance of boundary terms. We use the kernel freedom of the complex Langevin equation to push the breakdown to larger real-times. We search for the optimal kernel using machine learning methods. Thus, we extend the available range for 1+1d scalar simulations beyond the state of the art simulations.

*The 41st International Symposium on Lattice Field Theory (LATTICE2024)
28 July - 3 August 2024
Liverpool, UK*

*Speaker

1. Introduction

Understanding the dynamics of quantum systems requires the ability to calculate real-time correlators in such systems. This applies in many areas in theoretical physics, be it condensed matter physics, nuclear-, particle- physics or cosmology. However, such calculations currently rely on various approximation schemes, as a genuine non-perturbative ab initio approach remains unavailable. Lattice discretisation is a very successful ab initio approach to equilibrium physics (and static correlators), using the Euclidean-time formalism. In contrast, in the real-time formalism, the lattice has a very severe sign problem, hampering the usual Markov-chain Monte Carlo methods. This is a consequence of the fact that in the path-integral formalism, the weight of field configurations for real times is a phase factor.

Many approaches have been invented to circumvent the sign problem on the lattice, among others dual variables [1] which do solve the sign problem in certain cases, however their applicability is limited, extrapolation [2–5] and reweighting, which work as long as the sign problem is relatively mild, and there is a nearby ensemble with positive measure to use as a 'stand in' for the ensemble to be studied, and finally, methods using the analytic properties of the theory: complex Langevin [6, 7] and Lefschetz thimbles and related methods [8–11].

Quantum computers offer a different way to tackle the sign problem by e.g. building an analog quantum system in the quantum computer, such that unitary time evolution is realized. Currently interesting systems are out of the reach of quantum computers, however this might change in the future [12, 13].

Here we use the Complex Langevin equation (CLE) to tackle the sign problem. We study the time evolution of a scalar field with quartic interactions in 1+1 dimensions using the complex Langevin equation (CLE) [14]. A study of the same system using a Lefschetz-thimble inspired optimized manifold has appeared in [15], which we take as a benchmark calculation to assess the performance of the CL setup. The real-time scalar system in 0+1 dimensions as well as pure-gauge in 3+1 dimensions have been studied before using the CLE in [16, 17]. Recently it has been realized that using the Kernel freedom of the complex Langevin equation (which is similar to the introduction of a field dependent diffusion constant for the case of the real Langevin equation), one can influence the boundary terms and simulations for longer real-time extents are possible [18, 19]. To achieve this, one optimizes the kernel using a suitable loss function. Here we extend these studies to 1+1 dimensions, using the optimization procedure developed in the above mentioned two studies. In particular we deploy the highly efficient loss function proposed in [19].

In section 2, we shortly introduce the Complex Langevin equation with a kernel, in section 3 we describe our theory and our numerical setup, in section 4 we show numerical results.

2. Complex Langevin equation and Kernel

For scalar fields x_i , the Langevin equation reads as

$$dx_i = -\frac{\partial S}{\partial x_i} d\tau + 2dw_i \quad (1)$$

where dw is the increment of a standard Wiener process with $\langle dw_i = 0 \rangle$, $\langle dw_i dw_j \rangle = 2\delta_{ij} d\tau$, and $S(x_i)$ is the action.

The Langevin equation can be modified with a matrix H_{jk} , which can be an arbitrary function of the scalar fields.

$$dx_i = -H_{ji}H_{jk} \frac{\partial S}{\partial x_k} d\tau + \frac{\partial H_{ji}H_{jk}}{\partial x_k} d\tau + 2H_{ij}dw_j \quad (2)$$

One usually calls the matrix $K = H^T H$ the kernel. For the real Langevin equation, under rather mild assumptions, the stationary solution of the Fokker-Planck equation is unchanged under the introduction of a kernel. (The Fokker-Planck equation governs the Langevin-time evolution of the probability distribution $P(x_i, \tau)$.) For the CLE, in contrast to the real case, the stationary distribution on the complexified manifold does change. To ensure that the analytic continuation is not broken, we require the kernel to be a holomorphic function. In certain cases the introduction of the kernel can influence the appearance of the boundary terms [20, 21]. One observes that a kernel can in principle also cause the CLE to deliver incorrect results [18], recently understood to correspond to an integration cycle different than the desired real cycle (for details see [22]). We use boundary terms for diagnostic purposes, see [23, 24] for their definition and properties.

In this study we exploit the kernel degree of freedom to improve convergence properties, i.e. suppress boundary terms of the CLE by optimizing a kernel with machine learning methods, to be described in the next section.

3. Real-time scalar fields

We investigate a scalar field theory with quartic coupling, described by the action, written in Minkowski metric as

$$S = \int d^d x dt \frac{1}{2} \left((\partial_t \phi)^2 - (\partial_i \phi)^2 - m^2 \phi^2 - \frac{\lambda}{12} \phi^4 \right). \quad (3)$$

To describe temporal correlators such as $\langle \phi(t)\phi(0) \rangle$ we write in Heisenberg picture

$$\langle \phi(t)\phi(0) \rangle = \langle e^{i\hat{H}t} \phi e^{-i\hat{H}t} \phi \rangle \quad (4)$$

with \hat{H} the Hamiltonian of the system. In path-integral formalism, to describe this correlator, we need to define our theory on a Schwinger-Keldish contour, going first from $t = 0$ to some $t_{\max} \geq t$, then turning back and continuing from t_{\max} to $t = 0$, implementing the two time-evolution operators in the above formula. We can also describe thermal averages by using an imaginary time path at the end of the path so far, going from $t = 0$ to $t = -i\beta$ with the inverse temperature β , as well as choosing periodical boundary conditions on the fields: $\phi(t = 0) = \phi(-i\beta)$, implementing

$$\text{Tr}(e^{-\beta\hat{H}} \phi(t)\phi(0)) = \text{Tr}(e^{-\beta\hat{H}} e^{i\hat{H}t} \phi(t) e^{-i\hat{H}t} \phi(0)). \quad (5)$$

If we are interested in time ordered correlators, and since we have a time-independent Hamiltonian the second and third part of the contour can be replaced with any time-path starting at t_{\max} and ending at $-i\beta$. In practice we use a contour such that we split the vertical path in to two halves, one between the forward and backward branches and one at the end, as depicted in Fig. 1. We discretize

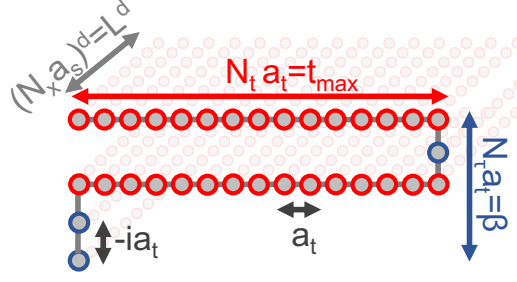


Figure 1: Geometry of discretized $(d+1)$ dimensional scalar field theory on the Schwinger-Keldysh contour. Here we use $N_t = 32$, $N_\tau = 4$ and $N_x = 8$ and $a_t m = 1/10$, $a_s m = 2/10$.

the 1+1 dimensional spacetime using the stepsize $a_s m = 0.2$ in spatial direction and $a_t m = 0.1$ in temporal direction. We discretise the action to yield

$$S = \sum_{n,k} a_s a_{t,n} \left[\frac{1}{2} \left(\frac{\phi_{n+1,k} - \phi_{n,k}}{a_{t,n}} \right)^2 + \frac{1}{4} \left(\left(\frac{\phi_{n,k+1} - \phi_{n,k}}{a_s} \right)^2 + \left(\frac{\phi_{n+1,k+1} - \phi_{n+1,k}}{a_s} \right)^2 \right) + \frac{1}{4} m^2 (\phi_{n,k}^2 + \phi_{n+1,k}^2) + \frac{1}{2 \cdot 4!} (\phi_{n,k}^4 + \phi_{n+1,k}^4) \right], \quad (6)$$

where $\phi_{n,k}$ is the scalar field on the discretised spacetime at the n -th time slice and k -th spatial point, and γ_n describes the discretised complex time-path, such that $a_{t,n} = \gamma_{n+1} - \gamma_n$.

To simulate the theory we use the kernelled complex Langevin equation (2), with a field independent matrix kernel. To optimize the matrix, we use Machine Learning inspired techniques, with the loss function (for more discussion see [14])

$$L = \int d^d x dt (\text{Im} \phi(x, t))^2. \quad (7)$$

4. Results

For numerical simulations we used $\lambda = 1$ and $\beta m = 0.4$ as also used in [15]. The lattice consisted of $N_t = 32$ points along the forward and backward branches of the contour and $N_\tau = 4$ along the vertical branch. We used $N_s = 8$ points along the spatial direction. Using temporal stepsize $a_t m = 0.1$ thus we have $t_{\max} = 3.2$, such that naive complex Langevin (i.e. using $H = 1$) breaks down on this contour due to large fluctuations and large boundary terms. We used an adaptively controlled Langevin update with maximal stepsize $\Delta\tau_{\max} = 0.001$.

Our observables are the equal time correlation function

$$F(\gamma) = \langle \phi(\gamma, p = 0) \phi(\gamma, p = 0) \rangle \quad (8)$$

and the unequal time two point function

$$C(\gamma) = \langle \phi(\gamma, p = 0) \phi(0, p = 0) \rangle. \quad (9)$$

Since the system is in thermal equilibrium, $F(t)$ is independent of the time, and it can also be measured on an imaginary time contour, $C(t)$ shows some nontrivial temporal dependence. Note

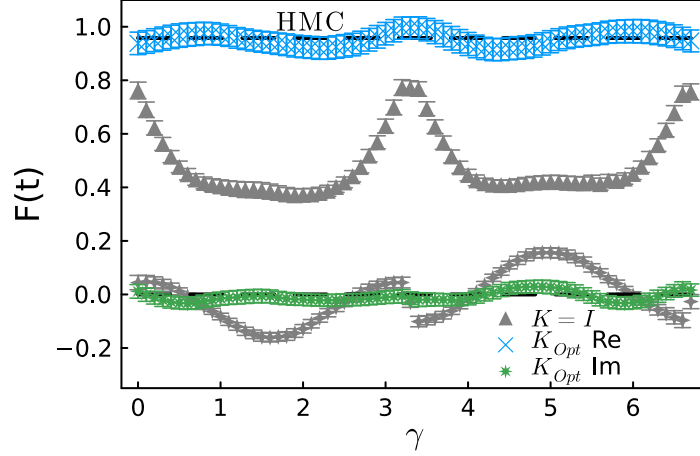


Figure 2: The equal time correlator defined in (8) as a function of the γ parameter indexing the points on the Schwinger-Keldysh-like contour. "HMC" shows the value of the correlator as calculated on an Euclidean time path. Grey symbols show naive CLE and blue and green symbols show results from CLE with the optimal kernel, as indicated.

that we have taken the zero momentum component in spatial directions, as this makes the correlator less susceptible to finite-size effects. In 0+1 dimensions one can easily calculate $F(t)$ and $C(t)$ using the Schrödinger equation [16], however introducing spatial directions makes that calculation very quickly infeasible.

The complex dense kernel is parametrized as $H = A + iB$ with two real matrices, which thus has $2((2N_t + N_\tau)N_s)^2$ parameters, where N_s is the number of lattice points in spatial direction, N_t is the number of time slices on the forward and backward branches, and N_τ on the vertical branch of the Schwinger-Keldysh contour. The gradients of the loss function are calculated by considering update steps using the current value of the kernel. In principle one update step suffices for this, but the autodiff capability of modern programming languages makes it easy to use many steps before taking the gradient. The optimization of H starts from a unit matrix, and we use a learning rate of 10^{-3} and the Adam optimizer. We observe a decay of the loss function from the $L \approx 1000$ initial value to $L \approx 7$ at the end of the optimization.

In Fig. 2 we show the measured equal time correlator for various setups. First of all, "HMC" shows the value of the correlator as measured on a sign-problem free imaginary time-contour. We also show the CLE results when using no kernel with grey triangles, and one observes that CLE gives clearly incorrect results in this case. Finally, we show the CLE results with an optimized kernel (blue and green symbols) and one observes time-independence, zero imaginary part and agreement with the "HMC" values, all of which are required from the correct solution. In Fig. 3 we show the measured values for $C(t)$ using the naive CLE as well as the CLE with the optimized kernel, as well as the HMC result for $C(0)$ shown with the dashed line. Also here, one notes that the two CLE results are inconsistent with each other. Since we must have $C(t=0) = F(t=0)$, we conclude that the naive CLE results are incorrect. The thimble result [15] is also shown with black symbols. The discrepancy at $t=0$ is likely the result of the slightly different UV cutoff used in that study (their a_t is double of the a_t we used in the CLE simulations). Note that the thimble calculation was not feasible for larger temporal extents due to high numerical costs. In contrast, the

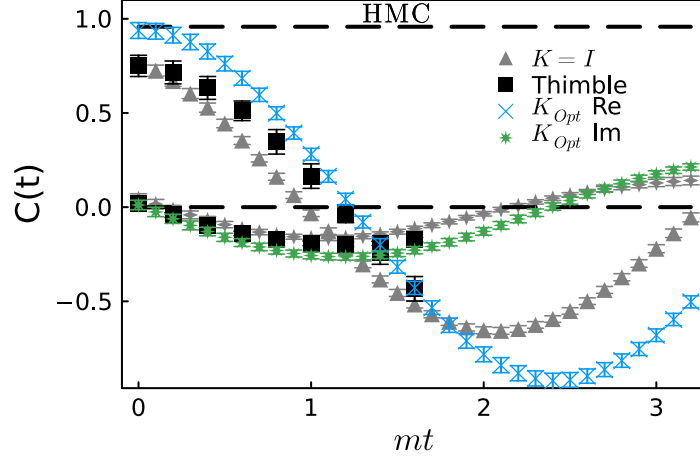


Figure 3: The unequal time correlator defined in (9). The "HMC" band shows the value of $C(0) = F(0)$ as measured on an imaginary time contour. Gray triangles show the results calculated with the naive CLE, blue and green symbols are calculate with the optimized kernel in the CLE. We also show the results from [15], for an identical system except that the temporal lattice spacing is double of that in the CLE calculations.

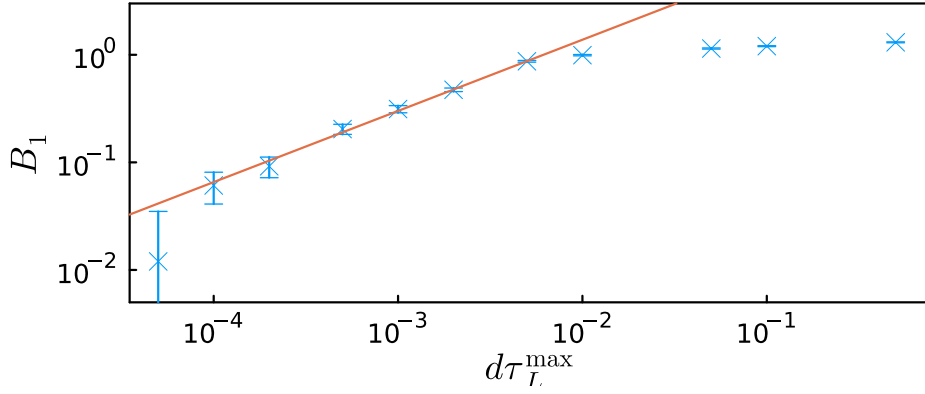


Figure 4: The boundary terms of ϕ^2 calculated in a CLE simulation with the optimized kernel, as a function of the maximal allowed stepsize in the adaptive stepsize algorithm.

CLE calculation uses a smaller temporal stepsize and has a t_{\max} twice as large, as our numerical costs grow in a much milder fashion when the volume of spacetime is increased. The agreement if $C(t = 0)$ suggests that our CLE results are correct. This is further corroborated by examining the boundary terms of the ϕ^2 observable. The boundary terms are known to be highly sensitive to finite stepsize effects, therefore we examine $B_1(\phi^2)$ as a function of the maximal Langevin stepsize in the adaptive control algorithm, as shown in Fig. 4. We observe a power-law decay such that in the continuum Langevin stepsize limit no boundary terms are expected.

Finally, in Fig. 5 we show the optimized kernel we used in the simulations to obtain Figs. 1 and 3. The color coding resolves almost all matrix values, except for the diagonal of the real part of the matrix, which is given by $\text{Re}[K_{\text{opt}} = 1.025]$. Each pixel corresponds to an element of the matrix such that the matrix index of the field $\phi_{n,k}$ is given by $i = k(2N_t + N_\tau) + n$ with $k = 0, \dots, N_s - 1$ and $n = 0, \dots, 2N_t + N_\tau - 1$. We observe that the real part of K_{opt} is dominated by the diagonal, while in the imaginary part one recognizes a banded structure differentiating between the branches

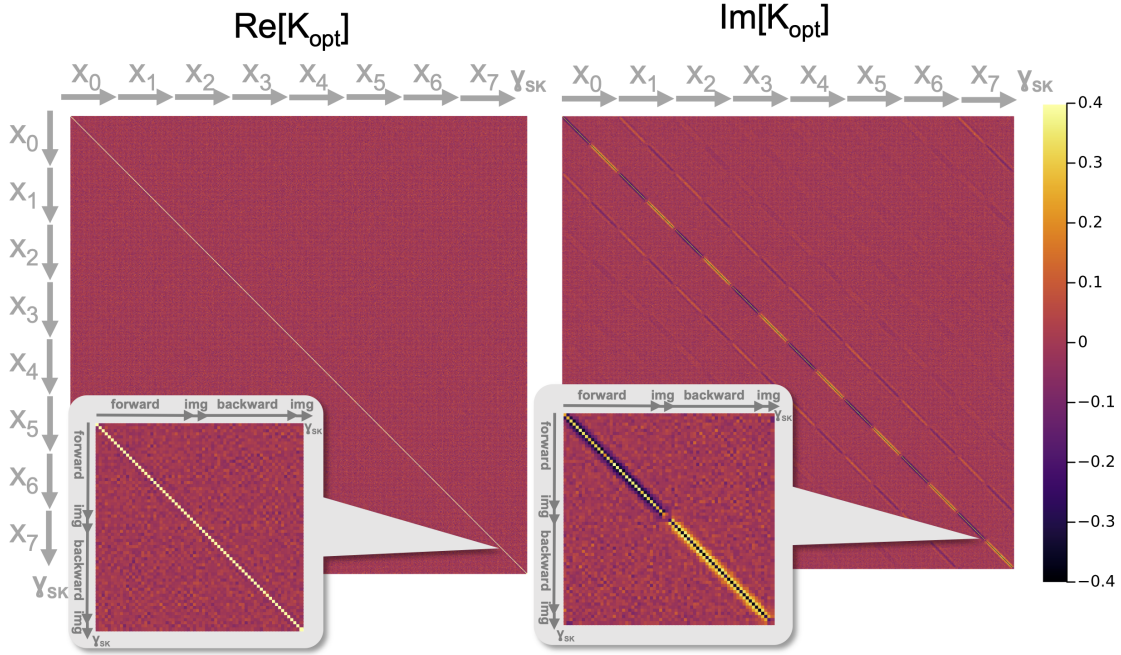


Figure 5: The heat-map of the real and imaginary parts of the optimized kernel of the CLE simulations. The points of the matrix are indexed such that the temporal coordinate is the fastest index. We also show a zoom-in to a single spatial slice.

of the contour. We generally see that non-diagonal values are small: the further away from the diagonal they are, the smaller values are observed. We also show an inset with a zoom in to a single spatial slice, where we note that a structure of the matrix is very similar to that observed in 0+1 dimensional calculations [18, 19].

5. Conclusions

In summary, we have shown that one can exploit the kernel freedom of the CLE to improve real-time simulations of scalar field theories. We used a dense constant matrix kernel in an 1+1 dimensional scalar field theory, and we have achieved correct simulations on time contours longer than what is available with other simulation methods. It is expected that further increasing the temporal extent will lead to an eventual failure as well, investigating the limit is an ongoing project. The most expensive part of the simulations is the training of the kernel, which we optimized with machine learning methods. We see various possibilities to improve upon the current result: First, we observe that a dense kernel is not needed to achieve convergence, and a sparser kernel (using e.g. a convolutional matrix) would most likely achieve the same benefits while having much reduced costs. Furthermore, it is expected that a field dependent kernel can be even more beneficial in reducing boundary terms at large temporal sizes. Lastly, extension of the idea to the more physically relevant 3+1 dimensions is also underway.

Acknowledgments

This research was funded in part by the Austrian Science Fund (FWF) via the Principal Investigator Project P36875. D. A. and A. R. received support from the Research Council of Norway under the FRIPRO Young Research Talent grant 286883. The study has benefited from computing resources provided by UNINETT Sigma2 - the National Infrastructure for High Performance Computing and Data Storage in Norway under project NN9578KQCDrtX "Real-time dynamics of nuclear matter under extreme conditions". Some parts of the numerical calculations were performed on GSC, the computing cluster of the University of Graz.

References

- [1] C. Gattringer and K. Langfeld, *Approaches to the sign problem in lattice field theory*, *Int. J. Mod. Phys. A* **31** (2016) 1643007 [[1603.09517](#)].
- [2] P. de Forcrand and O. Philipsen, *Constraining the QCD phase diagram by tricritical lines at imaginary chemical potential*, *Phys. Rev. Lett.* **105** (2010) 152001 [[1004.3144](#)].
- [3] J. Braun, J.-W. Chen, J. Deng, J.E. Drut, B. Friman, C.-T. Ma et al., *Imaginary polarization as a way to surmount the sign problem in Ab Initio calculations of spin-imbalanced Fermi gases*, *Phys. Rev. Lett.* **110** (2013) 130404 [[1209.3319](#)].
- [4] J. Braun, J.E. Drut and D. Roscher, *Zero-temperature equation of state of mass-imbalanced resonant Fermi gases*, *Phys. Rev. Lett.* **114** (2015) 050404 [[1407.2924](#)].
- [5] J.N. Guenther, R. Bellwied, S. Borsanyi, Z. Fodor, S.D. Katz, A. Pasztor et al., *The QCD equation of state at finite density from analytical continuation*, *Nucl. Phys. A* **967** (2017) 720 [[1607.02493](#)].
- [6] J.R. Klauder, *Stochastic Quantisation*, *Acta Phys. Austriaca Suppl.* **25** (1983) 251.
- [7] G. Parisi, *On Complex Probabilities*, *Phys. Lett. B* **131** (1983) 393.
- [8] N. Rom, D. Charutz and D. Neuhauser, *Shifted-contour auxiliary-field Monte Carlo: circumventing the sign difficulty for electronic-structure calculations*, *Chem. Phys. Lett.* **270** (1997) 382.
- [9] M. Cristoforetti, F. Di Renzo and L. Scorzato, *New approach to the sign problem in quantum field theories: High density QCD on a Lefschetz thimble*, *Phys. Rev. D* **86** (2012) 074506 [[1205.3996](#)].
- [10] A. Alexandru, G. Basar, P.F. Bedaque and N.C. Warrington, *Complex paths around the sign problem*, *Rev. Mod. Phys.* **94** (2022) 015006 [[2007.05436](#)].
- [11] J. Nishimura, K. Sakai and A. Yosprakob, *A new picture of quantum tunneling in the real-time path integral from Lefschetz thimble calculations*, *JHEP* **09** (2023) 110 [[2307.11199](#)].

- [12] C.W. Bauer et al., *Quantum Simulation for High-Energy Physics*, *PRX Quantum* **4** (2023) 027001 [2204.03381].
- [13] A.M. Dalzell et al., *Quantum algorithms: A survey of applications and end-to-end complexities*, 2310.03011.
- [14] D. Alvestad, A. Rothkopf and D. Sexty, *Lattice real-time simulations with learned optimal kernels*, *Phys. Rev. D* **109** (2024) L031502 [2310.08053].
- [15] A. Alexandru, G. Basar, P.F. Bedaque and G.W. Ridgway, *Schwinger-Keldysh formalism on the lattice: A faster algorithm and its application to field theory*, *Phys. Rev. D* **95** (2017) 114501 [1704.06404].
- [16] J. Berges, S. Borsanyi, D. Sexty and I.O. Stamatescu, *Lattice simulations of real-time quantum fields*, *Phys. Rev. D* **75** (2007) 045007 [hep-lat/0609058].
- [17] J. Berges and D. Sexty, *Real-time gauge theory simulations from stochastic quantization with optimized updating*, *Nucl. Phys. B* **799** (2008) 306 [0708.0779].
- [18] D. Alvestad, R. Larsen and A. Rothkopf, *Towards learning optimized kernels for complex Langevin*, *JHEP* **04** (2023) 057 [2211.15625].
- [19] N.M. Lampl and D. Sexty, *Real time evolution of scalar fields with kernelled Complex Langevin equation*, 2309.06103.
- [20] H. Okamoto, K. Okano, L. Schulke and S. Tanaka, *The Role of a Kernel in Complex Langevin Systems*, *Nucl. Phys. B* **324** (1989) 684.
- [21] K. Okano, L. Schulke and B. Zheng, *Kernel controlled complex Langevin simulation: Field dependent kernel*, *Phys. Lett. B* **258** (1991) 421.
- [22] M.W. Hansen, M. Mandl, E. Seiler and D. Sexty, *The Role of Integration Cycles in Complex Langevin Simulations*, 2412.17137.
- [23] M. Scherzer, E. Seiler, D. Sexty and I.-O. Stamatescu, *Complex Langevin and boundary terms*, *Phys. Rev. D* **99** (2019) 014512 [1808.05187].
- [24] M. Scherzer, E. Seiler, D. Sexty and I.O. Stamatescu, *Controlling Complex Langevin simulations of lattice models by boundary term analysis*, *Phys. Rev. D* **101** (2020) 014501 [1910.09427].